SolarPACES 2024, 30th International Conference on Concentrating Solar Power, Thermal, and Chemical Energy Systems

Advanced Materials, Manufacturing, and Components

https://doi.org/10.52825/solarpaces.v3i.2336

Published: 24 Nov. 2025

Enhancement of Compressive Strength of Perovskite FoamsUsed for Thermochemical Energy Storage

Mathias Pein[1,*], Asmaa Eltayeb[1], Artur Lang[1], Christos Agrafiotis[1], and Martin Roeb[1]

[1]Deutsches Zentrum für Luft- und Raumfahrt (DLR) e.V., Institute of Future Fuels, Germany

*Correspondence: Mathias Pein, mathias.pein@dlr.de

Abstract. Reticulated Porous Ceramics (RPCs), also known as ceramic foams are widely investigated for applications in Concentrated Solar Energy (CSE) harvesting, transformation, and storage. However, their inherent shape-related advantages - such as high gas-solid contact area and accommodation of high gas flow rates combined with low pressure drop due to their “open”, thin-struts-structure - are accompanied by low mechanical strength, which hinders large-scale, on-field applications. Foams prepared by the replica method - i.e. via impregnation of “sacrificial” polyurethane (PU) foam templates - exhibit hollow struts of about 100 µm thickness, which limit further their mechanical properties. In this work, an infiltration technique is presented that fills the hollow struts and substantially increases the mechanical strength of such RPC foam structures made of $Ca_{0.9}Sr_{0.1}MnO_3$ (CS10MO), a perovskite composition already identified as very promising for thermochemical storage of CSE. The developed infiltration technique achieves high degrees of infiltration and leads to a substantial increase of mechanical strength, specifically a 217% increase in withstandable compressive stress, from 0.23 MPa to 0.50 MPa. The results show that infiltration of hollow RPC foams can drastically increase the mechanical strength of prepared foam samples, not only making the open porous components for thermal storage devices more rigid and stable, but also increasing the envelope density by adding weight to the component within the same volume. Thereby, the applied infiltration simultaneously increases stability and volumetric storage density of a storage unit that utilizes such open porous foams.

Keywords: Perovskite, Ceramic Foam, Thermal Storage, Infiltration, Metal Oxide

1. Introduction

The transition to sustainable energy systems requires innovative materials that can efficiently store and release energy, particularly for applications such as thermal energy storage (TES). TES systems play a critical role in balancing energy supply and demand, enabling the storage of surplus energy during periods of low demand and its release during peak consumption. This provides potential benefits in areas such as long-term stability, cost and complexity compared to electrical energy storage units, e.g. batteries [1]. This capability is essential for integrating renewable energy sources, such as solar and wind, into the grid, given their inherent intermittency. Reliable thermal storage can be used to recover waste heat in high temperature industries [2] and is mandatory for concentrated solar energy facilities in order to supply electricity or process heat continuously (24/7), especially during nighttime [3].

Utilizing ceramics as sensible heat storage materials allows for TES at temperatures above 1000 °C, surpassing the capabilities of state-of-the-art molten salt or thermal oil heat storage units. Key factors in assessing a TES unit include total energy storage density, applicable mass flows of the heat transfer fluid as well as charge and discharge times. Open porous solids such as reticulated porous ceramics (RPCs), also known as ceramic foams, enable the use of air as the heat transfer fluid in direct contact with the storage material with minimal pressure drop [4]. More so, metal-oxides that can be reversibly reduced and oxidized in air can substantially increase the volumetric storage density by adding a chemical energy contribution to the sensible-only fraction, leading to thermochemical energy storage (TCES) process. In TCES, during the endothermal reduction by solar-heated air, additional heat is stored in the material, which is later released during subsequent exothermal oxidation. In the EU-funded project Restructure, DLR and its partners demonstrated this concept using cobalt oxide coated on extruded cordierite honeycombs [5]. Among the materials investigated for TCES, perovskites have garnered significant attention due to their unique structural properties, their high ionic conductivity and non-stoichiometric nature of their redox reactions. Perovskite oxides, particularly those based on calcium, strontium, and manganese, exhibit remarkable stability at high temperatures and a high degree of tunability in terms of their thermodynamic and structural properties. These characteristics make them promising candidates for TCES applications, where thermal stability, high energy storage capacity and efficient energy transfer are crucial. While monolithic structures made entirely from cobalt oxide were widely investigated [6,7,8], but were found to be thermomechanically unstable [9], recent work by the authors' group has shown that perovskites are suitable for the production of stable monolithic foams that withstand thermal cycling [10] and exhibit significant heat effects, which increase the storage density of a TES unit. These foams are produced by the so-called Schwartzwald or replica method, which employs a "sacrificial" polyurethane (PU) foam template, resulting in an RPC structure with interconnected struts [11]. However, these hollow struts can decrease the mechanical stability of the foam structures. One way to overcome this issue is to infiltrate the hollow struts with a filler material to enhance the rigidity of the resulting structures [12,13].

The presented work demonstrates the implementation of such infiltration techniques to perovskite foam structures for TCES and studies the effects on the mechanical properties of the RPC foams made from the perovskite material $Ca_{0.9}Sr_{0.1}MnO_3$. The results show an almost two-fold increase in their compressive strength.

2. Methods and Experimental Procedures

The synthesis, infiltration, and characterization of $Ca_{0.9}Sr_{0.1}MnO_3$ (CS10MO) RPCs were conducted using a systematic approach designed to optimize material properties for TCES applications. The methodologies employed can be broadly categorized into material synthesis, infiltration techniques, and comprehensive characterization.

2.1 Synthesis of $Ca0.9Sr0.1MnO_3$ Perovskite

The synthesis of $Ca_{0.9}Sr_{0.1}MnO_3$ powder was performed using a solid-state reaction method. The precursors $CaCO_3$ (>99%), $SrCO_3$ (>99%), and Mn_3O_4 (>98%) in stoichiometric ratios, were thoroughly mixed in isopropanol with subsequent filtering and drying. The mixed powders were then calcined at 1200 °C for 24h to produce single phase $Ca_{0.9}Sr_{0.1}MnO_3$, as confirmed by X-ray diffraction (XRD) analysis. The sintered perovskite powder was then processed in a ball mill (Fritsch Pulverisette 5) in ZrO_2 milling media to render its average size suitable for the preparation of stable slurries, targeted between 5-10 µm. Particle size was analyzed using a laser diffractometer (LA-960 Horiba Scientific Portica LA, Retsch Technology GmbH). The gained powder had a median particle size d_{50} = 6.7 µm.

2.2 RPC Framework Preparation and Infiltration

Perovskite RPCs were prepared using the replica method. Cylindrical PU templates (HSE-FoamTec GmbH, Germany) with dimensions ⌀35x40 mm were used to prepare samples designated for mechanical strength tests. The PU templates were immersed in a slurry of perovskite powder, which contained demineralized water, binder (Optapix PA 4 G, Zschimmer & Schwarz), and dispersant (Dolapix CE 64, Zschimmer & Schwarz) in weight percentages of 20%, 0.84%, and 1.5%, respectively, relative to the solid content. After removing excess slurry, the samples were dried for 24h in ambient air and subsequently fired in a single-stage process in a Nabertherm L08/17 BO muffle furnace. The foams were debinded at 553 K for 1 hour and 823 K for 1 hour, with a heating rate of 6 K/hour. The samples were then heated to 1623 K with a rate of 120 K/hour, and held at this temperature for 2 hours before cooling down to room temperature at a rate of 300 K/hour. Infiltration was performed by gradually pouring a slurry over the sintered foam bodies in an evacuated chamber (see **Figure 1**) in four stages, with 3 minutes of equilibration between each stage until the samples were fully immersed. Excess slurry was removed using pressurized air, and infiltrated samples were dried for 24h at ambient conditions. Subsequently, the dry, infiltrated samples were fired in a Carbolite Gero RHF 14/35 muffle furnace at 1573 K for 2 hours, with a heating rate of 300 K/h. All non-infiltrated samples went through identical temperature protocols to exclude sintering effects on the mechanical strength of the foams.

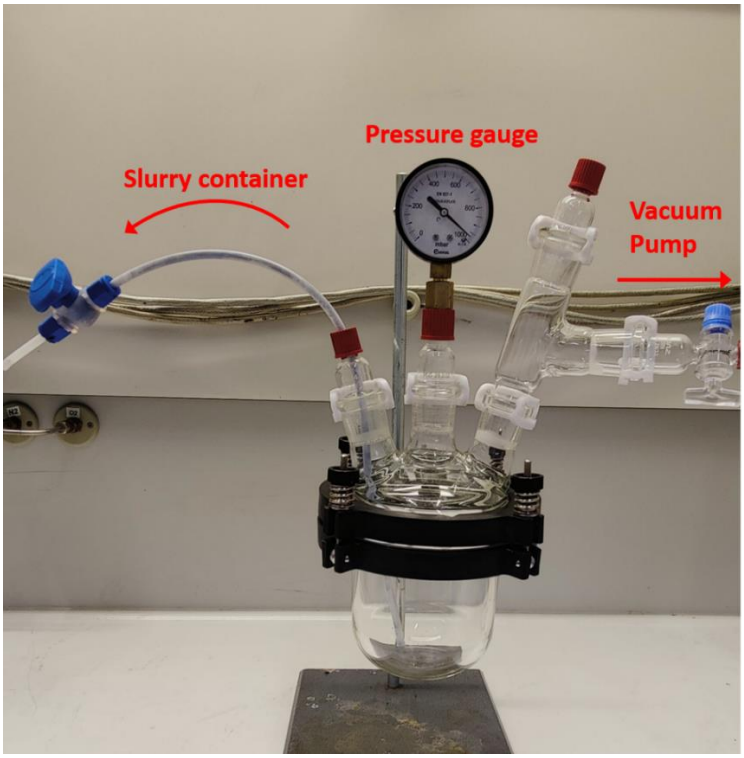

Figure 1. *Utilized infiltration setup*

2.3 Characterization Techniques

A range of characterization techniques was employed to evaluate the microstructural, thermal, and mechanical properties of the infiltrated RPCs:

Scanning Electron Microscopy (SEM): The microstructure of the infiltrated RPCs was analyzed using a Hitachi SU3900 electron microscope, provided detailed images of the infiltrated perovskite distribution within the foam framework.

X-ray Diffraction (XRD): XRD analysis was conducted with a Bruker D8-Advance X-ray diffractometer, equipped with a Co-X-ray radiation source and a LynxEye XE-T detector. Scans were performed in a θ − 2θ setup with diffraction angles (2θ) ranging from 10° to 100°, a step size of 0.02°, and a measurement time of two seconds per step.

Mechanical Testing: The mechanical properties of the infiltrated RPCs were evaluated through compressive strength tests using an Instron model 5566A universal testing machine, with a maximum load capacity of 10 kN. Alumina fleece was placed on top and bottom of each RPC sample to ensure a more uniform force distribution (see also **Figure 2**c).

3. Results and Discussion

All samples were made entirely from single phase $Ca_{0.9}Sr_{0.1}MnO_3$ (CS10MO) perovskite and were manufactured using a 10ppi (pores per linear inch) PU template. The resulting monolithic foam structures were both rigid and stable, providing a solid basis for further testing. The infiltration process was investigated using slurries with varying solid content, ranging from 60 wt.% - 75 wt.%. The most favorable results were obtained with a solid content of 65 wt.%. At solid contents higher than 65 wt.%, some clogging of pores and accumulation of slurry within the foam structure were observed, indicating that the infiltration process was less efficient. Conversely, at solid contents below 60 wt.%, insufficient infiltration was noted, resulting in incomplete filling of the hollow struts. Therefore, a solid content of 65 wt.% proved to be the most effective for achieving optimal infiltration of the hollow struts. Three samples in total have been prepared subsequently. Table 1 shows their weight increase after the infiltration.

Table 1. *Weight increase of 10ppi CS10MO foams infiltrated by 65 wt.-% slurry.*

Sample	Weight (pristine)	Weight (infiltrated)
CS10MO-01	25.17(1) g	33.20(1) g
CS10MO-02	24.02(7) g	31.56(2) g
CS10MO-03	25.71(0) g)	35.56(4) g

All the results presented in this work are based on CS10MO foam samples infiltrated with a slurry containing 65 wt.% solid content of perovskite powder and were obtained from sample CS10MO-03 given in Table 1. Pictures of the CS10MO foam samples used for mechanical testing are shown in **Figure 2**.

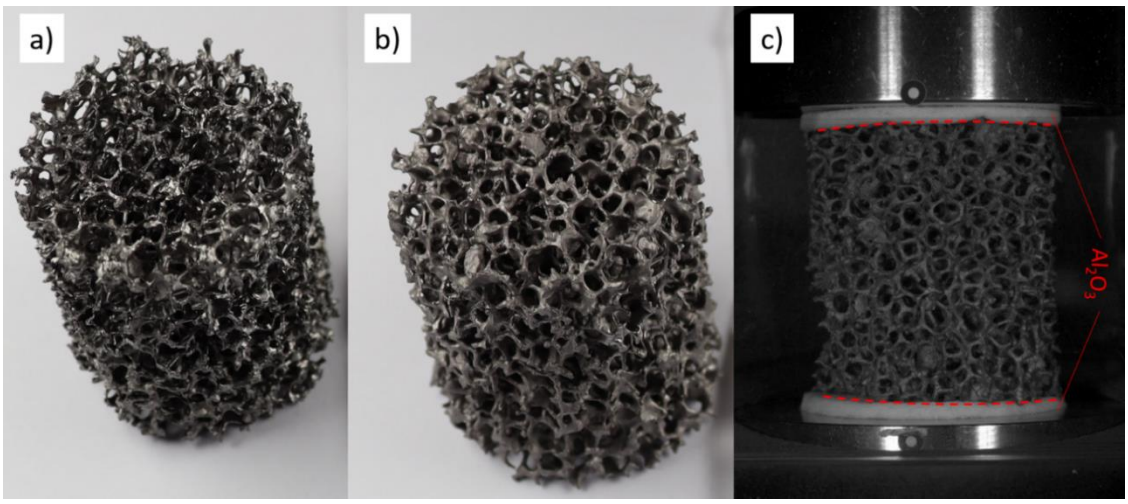

Figure 2. *Photographs of CS10MO 10 ppi foam samples used for compressive mechanical testing: a) non-infiltrated foam; b) infiltrated foam. c) Foam sample at the start of mechanical testing.*

After drying and sintering, the weight of the infiltrated sample had increased from 25.71(0) g to 35.56(4) g, an increase by 38.3% compared to the pristine sample. This weight increase did not solely originate from the infiltration of hollow struts of the foam, but also resulted from the formation of a thin additional coating layer on the exterior of the foam struts. This was confirmed through examination with an optical microscope. Close-up SEM micrographs of identical non-infiltrated and infiltrated samples are shown in **Figure 3** and **Figure 4**, respectively, highlighting the differences in structure and material distribution. In **Figure 3**, the hollow nature of the struts, resulting from the RPC manufacturing process, becomes evident. During the debinding and sintering stages of the foam production, the original PU template is burned off, leaving voids inside the struts that form the 3D foam structure.

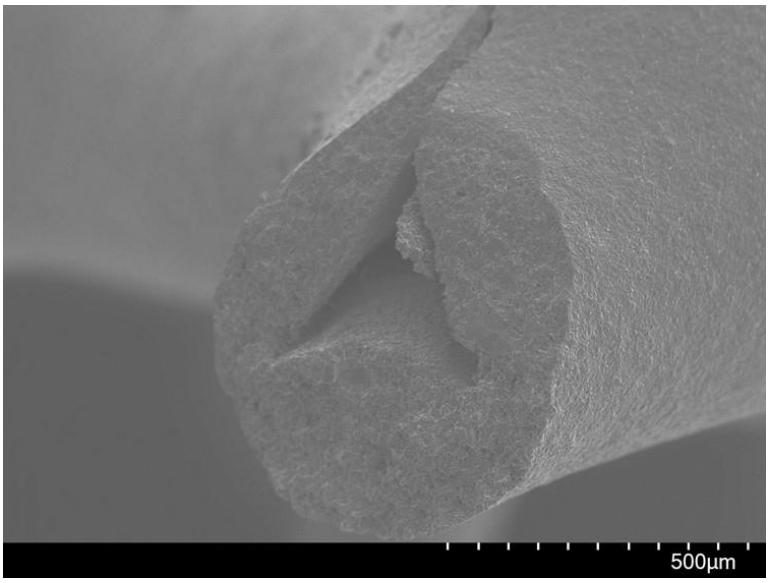

Figure 3. *SEM micrograph of a hollow strut from a non-infiltrated CS10MO foam.*

This network of voids and thin, hollow struts constitutes the overall 3D structure, that is relatively fragile under mechanical stress and load due to its inherent emptiness and thin walls. In contrast, **Figure 4** shows the infiltrated sample, where the struts are almost completely filled. This observation highlights the effectiveness of the presented infiltration procedure. The infiltration process results in a much denser backbone structure by filling the voids and reinforcing

the struts, thereby improving the structural integrity and load-bearing capacity of the foam. This enhancement is considered to significantly increase the mechanical strength of the foams.

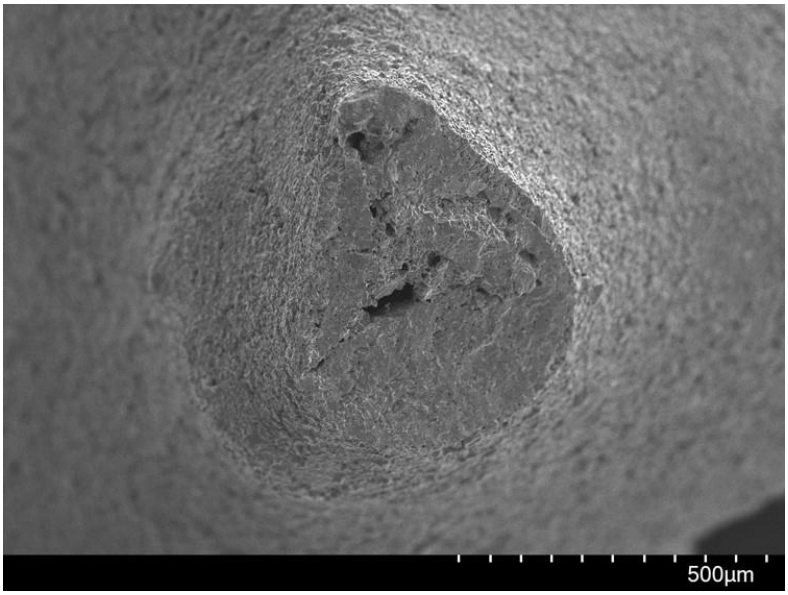

Figure 4. *SEM micrograph of a strut from an infiltrated CS10MO foam.*

At first glance, the infiltrated samples appear more rigid and stable. Mechanical strength was analyzed through compression tests, with the results for non-infiltrated and infiltrated CS10MO foam presented in **Figure 5** and **Figure 6**. The 'point of failure' was determined as the highest peak in withheld compressive force before the first cracks appeared. Typically, the foams do not collapse all at once; instead, individual struts break sequentially, leading to the formation of large cracks throughout the structure before a complete collapse occurs. The initial compressive deformation, during which the compressive force increases substantially, is primarily due to the compression of the alumina fleece used to enhance force distribution over the base area of the foam structure.

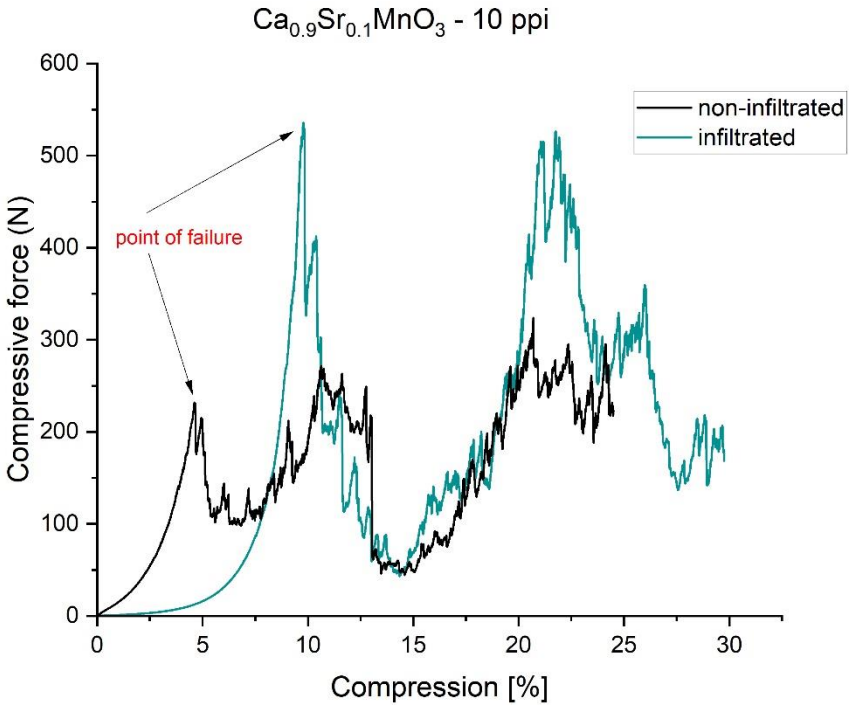

Figure 5. *Compressive force vs. compression of non-infiltrated and infiltrated CS10MO foam samples.*

The compressive force withheld by the infiltrated foam was 535.6 (+/- 2.7) N, representing a 231% increase compared to the non-infiltrated foam, which withstood only 231.8 (+/- 1.2) N. To facilitate better comparison, the compressive stresses were calculated (see Figure 6) based on the respective base areas of the infiltrated and non-infiltrated foams. It has to be considered that the calculated compressive stresses do not directly compare to values for bulk CS10MO, as only a fraction of the base area is effectively filled due to the highly porous nature of the foam structure.

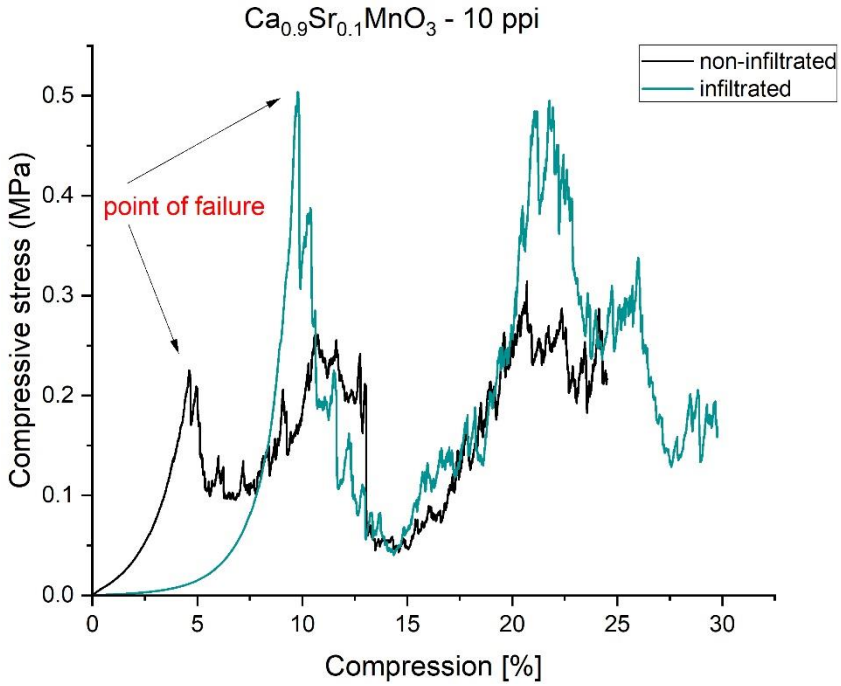

Figure 6. *Compressive stress vs. compression of non-infiltrated and infiltrated CS10MO foam samples.*

The maximum compressive stress that the foam samples were able to withstand before failure was 0.23 MPa for the non-infiltrated foam and 0.50 MPa for the infiltrated foam. Therefore, the infiltration process results in a 217% increase in compressive stress, reflecting more than a twofold improvement in compressive strength. These results are indeed very promising for the application of 3D open porous foam structures in thermochemical redox processes. Mechanical strength is substantial for the implementation of such structures, especially at scale where the compressive load from stacked modules becomes increasingly challenging to manage. Based on the presented results, infiltration is a viable procedure to strengthen 3D open porous perovskite foams. Additionally, while infiltration increases the weight of the foam by over 30%, this weight gain primarily results from filling the hollow struts and adding a thin coating layer. Despite this increase in weight, the porous structure of the foam is not severely altered. In fact, the infiltration enhances the volumetric density of the foam without major drawbacks in terms of porosity, pressure drop, or gas-solid reaction efficiency. This improvement could positively impact the thermal storage capacity of TESs as well as the round-trip capacity in air-separation units that employ such 3D foam structures.

4. Summary and Outlook

The presented work has successfully demonstrated the implementation of an infiltration process to fill the hollow struts of open porous 3D foam structures made from $Ca_{0.9}Sr_{0.1}MnO_3$ perovskite ceramics. The infiltration process was shown to increase the mechanical strength by over 200%, resulting in more rigid and mechanically stable foam structures. Importantly, the infiltration did not lead to the clogging of pores but increase the sample's weight by over one-

third, thereby raising the envelope density of the foam. This increase in envelope density is particularly beneficial for thermal storage applications, as it substantially enhances the volumetric storage density of such foam structures.

Ongoing work includes further analysis and comparative testing of infiltrated and non-infiltrated foams through porosity measurements using Hg-porosimetry and gas adsorption porosimetry, as well as pressure drop assessments. Additionally, the study will be extended to foams with higher pores per inch (ppi) to explore the effects on mechanical and thermal properties. Moreover, CT scans of non-infiltrated and infiltrated foam samples are planned to enable a more detailed calculation of the actual force distribution within the structure, which could lead to further enhancement of the mechanical stability of these structures.

Author contributions

Mathias Pein: conceptualization, methodology, visualization, resources, writing - original draft preparation, writing - review and editing, supervision, project administration; **Asmaa Eltayeb**: conceptualization, methodology, investigation, writing – review and editing, supervision, project administration; **Arthur Lang**: methodology, investigation, writing – review and editing; **Christos Agrafiotis**: resources, writing – review and editing, project administration, funding acquisition; **Martin Roeb**: resources, writing – review and editing, funding acquisition.

Competing interests

The authors declare that they have no competing interests.

Data availability statement

Data will be made available on request.

Funding

This work was performed within Project “HERCULES: High-temperature thermochemical heat storage powered by renewable electricity for industrial heating applications” that has received funding by the European Commission, through the HORIZON EUROPE, RIA – Research and Innovation Actions programme HORIZON-CL5-2022-D4-01-05 under grant agreement No 101104182.

References

[1] D. C. Stack, D. Curtis, and C. Forsberg. “Performance of firebrick resistance-heated energy storage for industrial heat applications and round-trip electricity storage”. Applied Energy 242, pp. 782–796, 2019.
[2] Kraftblock GmbH. Ed. by https://kraftblock.com/de/anwendungen/waste-heat.html. URL: https://kraftblock.com/de/anwendungen/waste-heat.html (accessed on 24/08/2024)
[3] L. Miró et al., “Thermal energy storage (TES) for industrial waste heat (IWH) recovery: A review”, Applied Energy, Volume 179, pp. 284-301, 2016.
[4] M. V. Twigg and J. T. Richardson. “Fundamentals and Applications of Structured Ceramic Foam Catalysts”. In: Industrial & Engineering Chemistry Research, 46.12, pp. 4166–4177, 2007.
[5] S. Tescari et al., “Experimental evaluation of a pilot-scale thermochemical storage system for a concentrated solar power plant”, Applied Energy, 189, pp.66–75, 2017.
[6] C. Pagkoura et al., “Cobalt oxide based structured bodies as redox thermochemical heat storage medium for future CSP plants”, Solar Energy, 108, pp. 146-163, 2014.

[7] C. Pagkoura, et al., “Cobalt Oxide Based Honeycombs as Reactors/Heat Exchangers for Redox Thermochemical Heat Storage in Future CSP Plants”, Energy Procedia, 69, pp. 978-987, 2015.
[8] G. Karagiannakis et al., “Cobalt/cobaltous oxide based honeycombs for thermochemical heat storage in future concentrated solar power installations: Multi-cyclic assessment and semi-quantitative heat effects estimations”, Solar Energy, 133, pp. 394-407, 2016.
[9] G. Karagiannakis et al., “Thermochemical storage for CSP via redox structured reactors/heat exchangers: The RESTRUCTURE project”, AIP Conference Proceedings 1850, 090004, 2017.
[10] M. Pein et al., ‘‘Reticulated porous perovskite structures for thermochemical solar energy storage’’, Advanced Energy Materials, 12(10), 2102882, 2022.
[11] M. Scheffler, P. Colombo (Editors), “Cellular Ceramics: Structure, Manufacturing, Properties and Applications, 2005 Wiley-VCH Verlag GmbH & Co. KGaA, 2005.
[12] I.-K. Jun et al., Reinforcement of a Reticulated Porous Ceramic by a Novel Infiltration Technique. Journal of the American Ceramic Society ;89(7):2317–9, 2006.
[13] U.F. Vogt et. al, Improving the properties of ceramic foams by a vacuum infiltration process. Journal of the European Ceramic Society ;30(15):3005–11, 2010.